

Above-barrier γ -ray emission by ultrahigh-energy electrons in oriented single crystals

Yu. V. Kononets

Kurchatov Institute Russian Science Center, 123182 Moscow, Russia

I. S. Tupitsyn

Royal Institute of Technology, S-100 44 Stockholm, Sweden

(Submitted 25 February 1994)

Pis'ma Zh. Eksp. Teor. Fiz. **59**, No. 8, 491–497 (25 April 1994)

The spectra of the γ -ray emission by ultrafast electrons in a thin crystal are analyzed theoretically for the case in which there is a strong competition between coherence effects and magnetobremstrahlung effects. This is the first such analysis. The properties of axial and planar coherence resonances which arise in the emission upon the transition from an axial orientation of the crystal to a planar orientation have been studied.

1. Recent CERN experiments¹ have revealed some new features in the γ -ray emission of ultrarelativistic electrons in crystals. Specifically, when the target orientation is changed from axial to planar, the emission spectra acquire some new peaks, in addition to the clearly defined, low-frequency peaks associated with the effect of the average force fields of the atomic planes of the crystal. These new peaks are intense, high-frequency peaks which stem from coherence effects involving nearby atomic rows (these are axial coherence resonances).¹⁾

We denote by θ the angle between the direction of the primary beam and the system of atomic rows of the crystal in which we are interested. In the most interesting interval of this angle,

$$\theta \sim \theta_d \equiv (2d/a_{TF})^{1/2} \theta_L, \quad (1)$$

in which the peaks of axial coherence resonances are particularly intense, the trajectory of the radiating particle deviates substantially from rectilinearity along the coherence length for the process. Consequently, to correctly describe the properties of the γ radiation under these conditions, we must go beyond the scope of the theory of coherent bremsstrahlung,^{3,4} which is based on the approximation of rectilinear trajectories. Here d is the distance between the coherently acting atomic rows, a_{TF} is the Thomas–Fermi screening length of an individual atom, and $\theta_L = (2U_0/E)^{1/2}$ is the Lindhard critical angle,⁵ which is determined by the depth (U_0) of the effective potential of the row and the energy (E) of the radiating electron.

2. In this letter we present some results found through exact evaluations of integrals over the time τ which constitute the general Baier–Katkov semiclassical formula:³

$$\frac{dI}{d\xi} = \frac{\alpha mc^3}{\pi \lambda_c} \xi \left\{ \int_0^\infty \left[1 + \frac{1 + (1-\xi)^2 \gamma^2}{4(1-\xi)} \frac{\gamma^2}{c^2} [\mathbf{v}_\perp(\tau) - \mathbf{v}_\perp(-\tau)]^2 \right] \frac{\sin f(\tau)}{\tau} d\tau - \frac{\pi}{2} \right\}, \quad (2)$$

$$f(\tau) = \frac{c}{\ell_c(\omega, E)} \left[2\tau + \frac{\gamma^2}{c^2} \left[\int_{-\tau}^{\tau} v_{\perp}^2(\tau') d\tau' - \frac{1}{2\tau} [\mathbf{r}_{\perp}(\tau) - \mathbf{r}_{\perp}(-\tau)]^2 \right] \right]. \quad (3)$$

Here ℓ_c is the coherence length of the process in which a γ ray with a frequency ω is emitted:

$$\ell_c(\omega, E) = 2\gamma\lambda_c(1 - \xi)/\xi, \quad \gamma = E/mc^2, \quad \xi = \hbar\omega/E. \quad (4)$$

We are using the standard notation for Planck's constant, the fine-structure constant, the velocity of light, and the mass and Compton wavelength of the electron.

The transverse coordinates $\mathbf{r}_{\perp}(\tau)$ and velocities $\mathbf{v}_{\perp}(\tau)$ obey the ordinary classical equations of motion of an electron with an energy E in the effective potential of the system of atomic rows. They satisfy the initial conditions

$$\mathbf{r}_{\perp}(0) = \mathbf{r}_{\perp}^0, \quad \mathbf{v}_{\perp}(0) = \mathbf{v}_{\perp}^0. \quad (5)$$

Expression (2) is usually interpreted as the frequency distribution of the γ rays emitted by the electron per unit time at the instant at which the point \mathbf{r}_{\perp}^0 is passed at a velocity \mathbf{v}_{\perp}^0 (this is a partial spectrum). The physically observable spectrum $d\bar{I}/d\xi$, for the radiation in a thin layer of a crystal, is found by integrating (2) over $d\mathbf{r}_{\perp}^0$ and $d\mathbf{v}_{\perp}^0$ with the distribution of electrons with respect to \mathbf{r}_{\perp}^0 and \mathbf{v}_{\perp}^0 .

3. The following points are important for understanding our results.

a) The partial spectra in the theory of coherent bremsstrahlung have a toothed structure, with jumps in the spectral functions at frequencies for which the following relations hold:

$$q_{\min}(\omega, E) = \mathbf{K}_{\perp} \cdot \mathbf{v}^0 / 2v^0, \quad (6)$$

where \mathbf{K}_{\perp} is an arbitrary vector of the 2D reciprocal lattice corresponding to the family of crystallographic axes under consideration, and $\hbar q_{\min}$ is the minimum momentum transferred to the crystal in the emission process²⁾:

$$q_{\min}(\omega, E) = A\ell_c^{-1}(\omega, E), \quad A = 1 + \frac{\gamma^2}{c^2} (\langle \mathbf{v}_{\perp}^2 \rangle - \langle \mathbf{v}_{\perp} \rangle^2). \quad (7)$$

The factor A determines a renormalization of q_{\min} associated with the mean square fluctuation of the electron velocity over the γ -ray formation length.³⁾

In the theory of coherent bremsstrahlung, there are strict correlations between the spatial and temporal Fourier components of the velocity \mathbf{v}_{\perp} (in using the word "spatial" here we have in mind the dependence on \mathbf{r}_{\perp}^0). Because of these correlations, and also because of our neglect of the \mathbf{r}_{\perp}^0 dependence of the renormalization of q_{\min} , the large family of intensity jumps in the integral spectrum disappears in the case of a uniform spatial distribution of the electrons. All that remains are the "teeth" corresponding to twice the reciprocal-lattice vector in Eqs. 6.

b) In a real physical situation, three factors—the variation in the electron velocity over the distance between neighboring atomic rows, the dependence of the renormalization of q_{\min} on the position of the electron trajectory in the crystal, and the disruption of the correlations (just mentioned) between the spatial and temporal Fourier

components of the electron velocity—should convert the intensity teeth in the integral spectrum into smooth peaks. “Antiresonance” structures with intensity minima may arise near frequencies which satisfy (6) with $\mathbf{K}_\perp/2 \neq \mathbf{K}'_\perp$.

c) Under the condition $\theta \lesssim \theta_0 \equiv U_0/mc^2$ the characteristic angle through which an electron is deflected in the field of an atomic row is $\Delta\theta \gtrsim \gamma^{-1}$, and the time scale ($\tau_\gamma = a_{TF}/c\theta_0$) of the deflection through an angle γ^{-1} is independent of both θ and γ . Under these conditions the main frequencies of the axial coherent resonances satisfy

$$q_{\min}^{-1}(\omega, E) = c\tau_\gamma\theta_*/\theta, \quad \theta_* \equiv \theta_0 d/2\pi a_{TF}, \quad (8)$$

which shows that at $\theta \lesssim \theta_*$ the shaping of the peaks of the axial coherence resonances is subjected to a strong influence of magnetobremstrahlung effects. Two conclusions obviously follow: 1) The renormalization of q_{\min} depends only weakly on γ and θ ; this dependence is governed by the time τ_γ (a simple estimate yields an effective value $A \simeq 5/4$). 2) The intensification of the peaks of the axial coherence resonances with increasing γ under the condition $\gamma\theta = \text{const}$ is weaker than predicted by the theory of coherent bremsstrahlung, and the magnetobremstrahlung tendencies in the “background” part of the spectrum are strengthened.

4. Since the competition between magnetobremstrahlung and coherence effects should be most obvious in crystals of heavy elements, we carried out some specific calculations of the emission spectra for electrons with energies from 75 GeV to 4.8 TeV in a Ge single crystal in the $\langle 110 \rangle$ orientation at a temperature $T = 293$ K. We considered a range of angles of incidence corresponding to a transition from a $\langle 110 \rangle$ axis orientation of the target to a $\{001\}$ -plane orientation.

The potential of the interaction between the electrons and the system of $\langle 110 \rangle$ atomic rows of the crystal is described by a superposition of Doyle–Turner potentials averaged over the temperature.⁶ In accordance with Ref. 7, we set the 1D amplitude of the thermal vibrations of the Ge atoms at $T = 293$ K equal to $u_1 = 0.0829$ Å. The basic parameters characterizing this physical situation are

$$\theta_0 = 4.3 \times 10^{-4} \text{ rad}, \quad a_{TF} = 0.1476 \text{ Å}, \quad d = 4.0008 \text{ Å}, \quad b = 1.4145 \text{ Å}. \quad (9)$$

Here d is the distance between the $\langle 110 \rangle$ atomic rows in a $\{001\}$ plane, and b is the distance between $\{001\}$ planes.

In the numerical integration of the equations of the transverse motion, we used the initial conditions in (5) with $v_{1x}^0 = c\sin\theta\cos\varphi$ and $v_{1y}^0 = c\sin\theta\sin\varphi$, where φ is the azimuthal angle, which specifies the direction of the uniform incident electron beam and which is reckoned from the $\langle 1\bar{1}0 \rangle$ direction in the $\{110\}$ plane (see the orientation diagram in the upper part of Fig. 1b). The computation algorithm is based on the idea that over a long time $|\tau| \gtrsim \tau_* \gg \ell_c/c$ the details of the force field are irrelevant, and the incident particle can be treated as free. The value of τ_* is determined by the error of the calculations. For the spectral curves in Figs. 1 and 2, this error is less than 2% over the main frequency range.

5. The series of curves in Fig. 1a shows the γ emission spectra as a function of the angle θ for the case in which a beam of electrons with $E = 300$ GeV is incident along a direction parallel to the system of $\{001\}$ planes ($\varphi = 0$). An exact calculation for

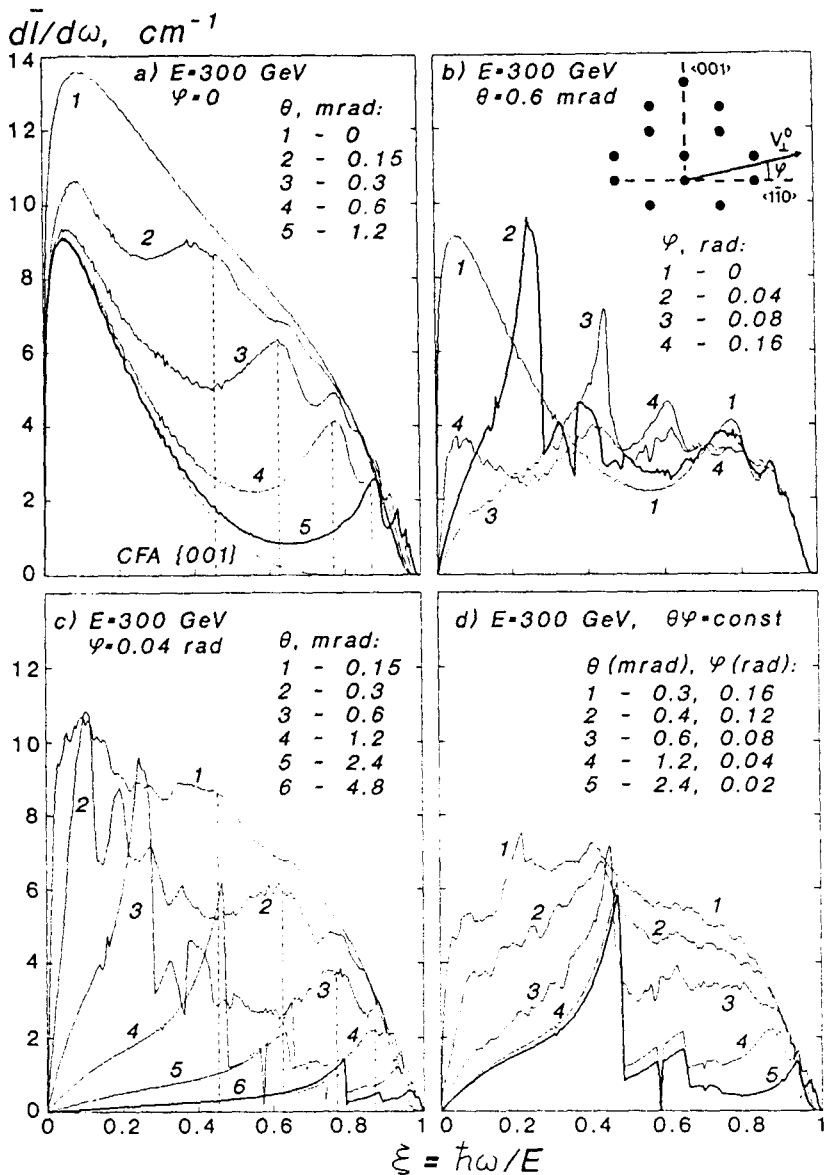


FIG. 1. Spectra of the γ rays emitted per unit path length as a function of the direction of the beam of electrons, with an energy $E=300$ GeV, in a Ge single crystal in the $\langle 110 \rangle$ orientation at $T=293$ K. a—CFA peaks and axial resonances for the case in which electrons are incident in a direction parallel to the $\{001\}$ planes; b—disappearance of the axial resonance and change in the structure of the $\{001\}$ -plane resonances with increasing value of the angle φ at $\theta=6 \times 10^{-4}$ rad (the inset at the upper right is a schematic diagram of the orientation of the initial transverse velocity of the electrons in the 2D lattice of the $\langle 110 \rangle$ -axis system); c— γ -emission spectra as a function of θ at $\varphi=0.04$ rad; d—shape of the $\{001\}$ -plane resonances as a function of the orientation of the electron beam for a fixed value of the product $\varphi\theta$ ($\varphi\theta=4.8 \times 10^{-5}$ rad²).

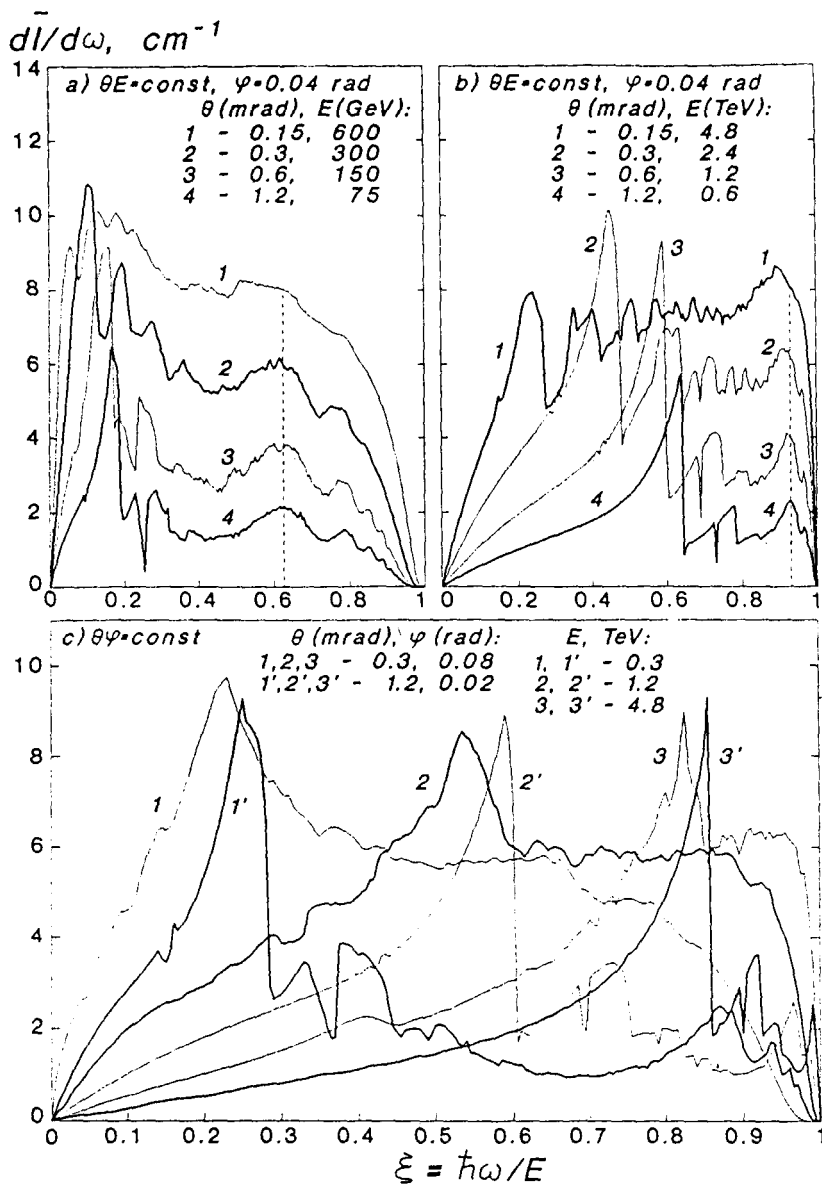


FIG. 2. Theoretical results, for the same target, which demonstrate magnetobremstrahlung effects in the spectra of coherence resonances (see the text proper for more details). a—Spectra of γ rays for several orientations of the electron beam, with $\varphi = 0.04 \text{ rad}$ and at a fixed value of the product θE ($\theta E = 0.09 \text{ rad} \cdot \text{GeV}$), in the electron energy range $E = 75\text{--}600 \text{ GeV}$; b—for the same orientations of the electron beam, but with $\theta E = 0.72 \text{ rad}$, in the interval $E = 0.6\text{--}4.8 \text{ TeV}$; c—structure of $\{001\}$ -plane resonances in the spectra of emitted γ rays versus the orientation and energy of the electron beam for the fixed value $\varphi\theta = 2.4 \times 10^{-5} \text{ rad}^2$.

$\theta=0$ yields a spectrum (curve 1) which coincides (within the calculation error) in the main frequency range with the spectrum calculated in the approximation of a constant field³ (CFA). Curves 2 and 3 demonstrate a rapid increase in the quantitative discrepancies with the CFA results with increasing θ at $\theta \lesssim \theta_0$; these curves also show how the peaks of the axial coherence resonances are formed under these conditions.

With a further increase in θ (curves 4 and 5), the low-frequency parts of the spectra approach the dashed curve, which shows the CFA spectrum in the average potential of the {001} atomic planes.

The shape of the smooth peaks of the axial coherence resonances is radically different from that of the sharp teeth of the sawtooth spectra of the theory of coherent bremsstrahlung. The positions of the crests of these peaks are described well by the formula

$$\xi_{ax}^{(i)} = (1 + A_{ax}d/4\pi i \lambda_c \gamma \sin \theta)^{-1}, \quad i=1, 2, \dots, \quad (10)$$

with a constant $A_{ax}=1.282$ [the points on the ξ axis which satisfy (10) are marked with dashed vertical lines]. This point demonstrates that *the effective renormalization of q_{min} for the peaks of the axial coherence resonances are essentially independent of θ over a θ interval significantly wider than⁴⁾ θ_0 .*

It is clear from simple physical considerations that under the condition

$$|\varphi| > \varphi_* \equiv a_{TF}/d \quad (11)$$

the peaks of the axial coherence resonances should be "painted over." The curves in Fig. 1b show that under the condition $|\varphi| \leq \varphi_* \approx 0.04$ the shape of the peaks of the axial coherence resonances is only negligibly different from that in the case with $\varphi=0$, but the peaks of the axial coherence resonances disappear completely as early as $|\varphi|=2\varphi_*$, giving way to a smooth distribution.

6. As $|\varphi|$ increases from zero, the smoothing of the peaks of the axial coherent resonances is accompanied by a substantial restructuring of the spectrum at low frequencies, at which the CFA planar peaks are replaced by *planar coherence resonances*, which result from the coherent effect of neighboring {001} planes.

At small values of φ , the peaks of the planar coherence resonances coexist with peaks of axial coherence resonances (Fig. 1b-d). In the case $\theta > \theta_0$ their properties correspond more closely to those of the intensity teeth from the theory of coherent bremsstrahlung. Their right-hand fronts are characterized by an abrupt intensity decay at the frequencies

$$\xi_{pl}^{(i)} = [1 + A_{pl}(\theta, \varphi)b/4\pi i \lambda_c \gamma \sin \psi]^{-1}, \quad \sin \psi = \sin \theta \sin \varphi, \quad i=1, 2, \dots, \quad (12)$$

where ψ is the angle between the direction of the electron beam and the {001} plane. The quantity A_{pl} tends rapidly toward one with increasing ψ : $A_{pl}-1 \propto \psi^{-2}$. This tendency is confirmed by the positions of the jumps on the curves in Fig. 1c, where we can clearly trace the transition to the results of the standard theory of coherent bremsstrahlung at large values of ψ .

In accordance with the discussion in Sec. 3b above, we can clearly see some narrow antiresonance dips in the spectra of the planar coherence resonances (Fig. 1c)

to angles $\theta = 2.4 \times 10^{-3}$ rad. These dips are at frequencies corresponding to half-integer values of i in (12). They are particularly obvious in the case $i = 3/2$. Their widths increase with decreasing θ . At the same time, the crests of the peaks of the planar coherence resonances become progressively rounder, and at $\theta \lesssim \theta_0$ the shape of the spectrum in the region of the planar coherence resonances and the emission intensity at the maxima and minima differ substantially from the predictions of the modified theory of coherent bremsstrahlung.

Significantly, the clearly defined peaks of planar coherence resonances continue to exist at $|\varphi| > 2\varphi_*$ (Fig. 1b), i.e., under conditions such that the "axial discreteness" of the structure of the {001} planes has a strong effect on the transverse motion of the radiating electrons, erasing the peaks of the planar coherence resonances. The physical explanation for this result is that the properties of the planar coherence resonances reflect only the characteristics of the electron motion averaged along the system of planes under consideration.⁵⁾

At a fixed value of γ , and at small angles, the positions and magnitudes of the intensity jumps of the planar coherence resonances depend on only $\psi = \varphi\theta$ in the theory of coherent bremsstrahlung. Figure 1d shows the sharply strengthening role of magnetobremsstrahlung effects with decreasing θ in the region $\theta \lesssim \theta_0$ under the condition $\varphi\theta = \text{const}$. As a result, there is a significant decrease in the size of the teeth of the planar coherence resonances, and these teeth become broader; the intensity of the background part of the spectrum increases. These changes occur in such a way that the total intensity of the radiation at the frequency of the main peak of the planar coherence resonances changes only slightly. There is some shift of the peak down the frequency scale, because of an increase in the fluctuations of the electron velocity. The general nature of this behavior of the peaks of the planar coherence resonances over a broad range of values of γ is confirmed by the spectral curves in Fig. 2c.

7. The results in Fig. 2 point out the following basic aspects of the above-barrier γ -ray emission at $\theta \lesssim \theta_0$:

a) The effective renormalization of q_{\min} at the frequencies of the axial coherence resonances is approximately constant, while that at the frequencies of the planar coherence resonances has a strong angular dependence.

b) The intensification of the peaks of axial coherence resonances with increasing γ at a fixed value of the product $\gamma\theta$ is far weaker than in the theory of coherent bremsstrahlung.⁶⁾

c) An increase in γ at fixed values of θ and φ shifts the peaks of the axial and planar coherence resonances toward the high-frequency edge of the spectrum in accordance with (10) and (12), respectively, with slight changes in the maximum intensity values.

d) Even at θ values considerably smaller than θ_0 , there is a fairly broad region of values, $|\varphi| \lesssim 2\varphi_*$, in which there is a pronounced suppression of the emission at low frequencies, $\xi < \xi_{\text{pl}}^{(1)}$, due to the planar coherence. This suppression becomes greater as γ -ray emission increases. An increase in γ -ray emission tends to concentrate the radiation energy at the high-frequency edge of the spectrum.

We do not have space here to go into detail on other interesting aspects of the γ -ray spectra. The reader can see these aspects in Fig. 2, where the dashed vertical lines show the positions of the peaks of the axial coherence resonances calculated from (10) with the same value of A_{ax} as for Fig. 1.

We note in conclusion that the most important aspects of the γ -ray emission by ultrafast electrons in crystals established above, in the case of a strong competition between coherence effects and magnetobremstrahlung effects, are amenable to experimental tests at the present state of the art.

This study had financial support from the Russian Basic Research Foundation (Project 93-02-2590).

- ¹⁾ Related effects have been seen in a theoretical analysis of the spectra of the photoproduction of e^+e^- pairs² in a corresponding physical situation.
- ²⁾ The jump in the partial spectrum thus indicates that the excess momentum which arises in the emission process at the frequency of the jump "is carried off" by half of a reciprocal-lattice vector. The partial spectral functions, which are not physically measurable quantities, are not positive definite. They have "intensity" jumps of arbitrary sign.
- ³⁾ The standard theory for coherent bremsstrahlung ignores the renormalization of q_{min} . The modified version of this theory,³ which incorporates a renormalization of q_{min} through the introduction of an effective electron mass m_* , "does not notice" that the coefficients A for the coexisting axial and planar coherence resonances (more on this below) are greatly different because of a difference in the effective time intervals over which the velocity fluctuations are averaged in A .
- ⁴⁾ In the modified theory for coherent bremsstrahlung we have $A_{ax} - 1 \propto (\theta_0/\theta)^2$. This behavior would lead to a pronounced shift of the peaks of the axial coherent resonances on curves 2 and 3 in Fig. 1a in the direction of lower frequencies. The value $A_{ax} = 1.282$ correlates well with the estimate $A_{ax} \approx 5/4$ mentioned above (in Sec. 3c). The region in which A remains constant broadens because the parameters in (9) correspond to $\theta_* = 4.3\theta_0 > \theta_0$.
- ⁵⁾ If, under the condition $|\varphi| > \varphi_*$, the electron beam is directed nearly parallel to a system of atomic planes of higher index, then at low frequencies a CFA peak and a peak of an axial coherence resonance corresponding to this high-index system of planes may appear to the left of the {001}-plane resonance. A situation of this sort is realized in Figs. 1b and 1d (curves 4 and 1, respectively).
- ⁶⁾ Since A_{ax} is constant, it is easy to show that the modified theory of coherent bremsstrahlung predicts an emission intensity which is linear in γ at the frequencies of the axial coherence resonances under these conditions.

¹R. Medenwaldt *et al.*, Phys. Lett. B **281**, 153 (1992).

²Yu. V. Kononets and I. S. Tupitsyn, JETP Lett. **57**, 151 (1993).

³V. N. Bañer *et al.*, *High-Energy Electromagnetic Processes in Oriented Single Crystals* [in Russian] (Nauka, Novosibirsk, 1989).

⁴M. A. Ter-Mikaelyan, *Effect of the Medium on High-Energy Electromagnetic Processes* [in Russian] (Izd. Akad. Nauk ArmSSR, Erevan, 1969).

⁵J. Lindhard, K. Danske Vidensk. Selsk. Mat.-Fys. Medd. **34**, No. 14 (1965).

⁶P. A. Doyle and P. S. Turner, Acta Crystallogr. A **24**, 390 (1968).

⁷O. H. Nielsen and W. Weber, J. Phys. C **13**, 2449 (1980).

Translated by D. Parsons